Bioorganic & Medicinal Chemistry 22 (2014) 6503–6508

Contents lists available at ScienceDirect

Bioorganic & Medicinal Chemistry

journal homepage: www.elsevier.com/locate/bmc

Microwave-assisted synthesis of phenanthroimidazole derivatives as stabilizer of *c-myc* G-quadruplex DNA

Siyan Liao [a], Zhao Zhang [b], Qiong Wu [b], Xicheng Wang [c,*], Wenjie Mei [b,*]

[a] Department of Chemistry, School of Pharmaceutical Sciences, Guangzhou Medical University, Guangzhou 510182, PR China
[b] School of Pharmacy, Guangdong Pharmaceutical University, Guangzhou 510006, PR China
[c] The First Affiliated Hospital of Guangdong Pharmaceutical University, Guangzhou 510006, PR China

ARTICLE INFO

Article history:
Received 17 July 2014
Revised 23 August 2014
Accepted 2 September 2014
Available online 28 September 2014

Keywords:
Phenanthroimidazole derives
c-myc G-quadruplex DNA
π–π stacking
Molecular docking

ABSTRACT

c-myc G-quadruplex DNA, which plays a central role in tumor progression and resistance, has been extensively investigated as potential target of antitumor drugs. In this paper, a series of phenanthroimidazole derives have been synthesized under irradiation of microwave in yields of 51–80%. The antitumor activity of these compounds against various tumor cells has been evaluated, and the results show that these compounds exhibit great inhibition to MDA-MB-231, MCF-7 and Hela cells, especially **5** inhibit the growth of MDA-MB-231 cells with IC_{50} about 3.6 μM. The further studies show that **5** can bind and stabilize *c-myc* G4 DNA in π–π stacking mode, which confirmed by the hypochromise in the electronic spectra of **5** with the increasing of *c-myc* G4 DNA. When dealt with **5**, the strength of CD signal attributed to *c-myc* G4 DNA is decreased and the FRET melting point of *c-myc* G4 DNA is increased. Moreover, the molecule docking calculation was conducted to show that **5** suitably stack onto the 5′ G-quartet surface, and parallels to the surfaces of the G5 and G-quartet consisting of G7, G11, G16, and G20. As a result, the replication of *c-myc* oligomers is blocked by **5**. In a word, this type of phenanthroimidazole derives can act as potential inhibitor against breast cancer cells by binding and stabilizing *c-myc* G4 DNA through π–π stacking.

1. Introduction

Oncogene *c-myc*, which is over-expression in a wide variety of human cancers, plays a critical role as a regulator of gene transcription involved in cell proliferation, cell division and metabolism.[1–3] The promoter region of *c-myc* oncogene are G-rich single-strand DNA and can form G-quadruplex structure via Hoogsten hydrogen bond in the presence of potassium and sodium ion.[4,5] It's reported that ligands that stabilize the *c-myc* overhang into G-quadruplex can be considered as potential antitumor agents to block the replication of *c-myc*. Various of small molecules, such as porphyrins, quindoline derivatives, carbamide analogs and quarfloxin, have been described to bind to *c-myc* G-quadruplex DNA and down-regulate the expression of C-MYC protein.[6–9] Some of these derivatives have been found to induce the apoptosis of tumor cells by stabilizing *c-myc* G-quadruplex structure.[10] Thus, it's been developed to be a promising strategy for the treatment of cancer by stabilizing G-quadruplex structure to suppression activity of *c-myc*.

Phenanthroimidazole derivatives with enlarged aromatic rings, which can bind to DNA through π–π stacking, are a type of classic DNA intercalators. There are number of evidence to show that this type of compound have wide applications as DNA-structural probe, molecular 'Light Switch', DNA-photocleavage reagent and antitumor drugs for their unique electrochemical and photophysical properties.[8] In our previous works, it's found that imidazo[4,5*f*][1,10]phenanthroimidazole derivatives can inhibit effectively the growth of human lung cancer A549 cells and induced tumor cells apoptosis, and down-regulate the expression of C-MYC protein by this compound have also been observed.[11] However, it's still not clear whether phenanthroimidazole derives can inhibit the growth of tumor cells through stabilized the G-quadruplex structure of *c-myc* promoter, and it's very important to design novel candidate with high activity and selectivity to tumor cells.

In this paper, a series of phenanthroimidazole derivatives (Fig. 1) have been synthesized with yield of 87% under microwave irradiation.[12] It's found that this class of compounds, especially **5** can inhibit the growth of various tumor cells, especially MDA-MB-231 cells. The binding behavior of **5** with *c myc* G4 DNA have been investigated by spectroscopy methods, FRET and PCR-stop assay, and the results show that **5** can stabilize the G-quadruplex structure and inhibit the replication of *c-myc* oligomers. This has been further confirmed by the molecular docking calculation to suggest that **5** may bind to *c-myc* G4 DNA via π–π stacking in an intercalating mode.

* Corresponding authors.
E-mail addresses: 13902400598@126.com (X. Wang), wenjiemei@126.com (W. Mei).

http://dx.doi.org/10.1016/j.bmc.2014.09.003
0968-0896/

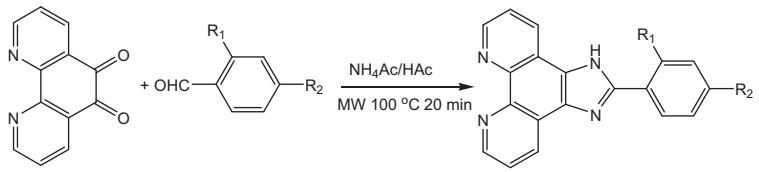

1 R_1=-H R_2=-H **2** R_1=-SO_3H R_2=-H **3** R_1=-H R_2=-SO_3H
4 R_1=-Br R_2=-H **5** R_1=-H R_2=-Br

Figure 1. Synthesis route of phenanthroimidazole derivatives under the irradiation of microwave.

2. Chemicals and methods

2.1. Chemicals

All reagents and solvents were purchased commercially and used without further purification unless specially noted. Distilled water was used in all experiments. *c-myc* oligomers strand 5′-TGAGGGTGGGTGGGTAA-3′ was purchased from Sangon Biotech and formed G-quadruplex conformation as literature by renaturation for 24 h at 4 °C, after denaturation for 5 min at 90 °C.[13,14] All aqueous solutions were prepared with doubly distilled water. The Tris-HCl buffer consisting of Tris and KCl, and the pH value was adjusted to 7.2 by HCl solution, which was applied to UV titration, Real time PCR (Biored IQ5) and CD spectra.

2.2. Physical measurements

The phenanthroimidazole derivatives were synthesized by using Anton Paar monowave 300 microwave reactor. ESI-MS spectra were obtained in methanol on Agilent 1100 ESI-MS system operating at room temperature. UV–vis absorption spectra were recorded on a Shimadzu UV-2550 spectrophotometer using 1 cm path length quartz cuvettes (3 mL). Circular dichroism (CD) spectra were operated on a Jasco J810 spectropolarimeter. Molecular docking data were calculated by using Addsol, Autogrid and Auto Tors tool of the software. FRET assay were determined with a Bio-Radi Q5 realtime PCR detection system. PCR-stop assay were operated on AlphaSC Thermal Cycler.

2.3. Synthesis of imidazole[4,5*f*][1,10] phenanthroline derivatives

Phenanthroimidazole derivatives were synthesized according to the literature procedure with some modification. In general, a mixture of 1,10-phenanthroline-5,6-dione (1.50 mmol), benzaldehyde (2.25 mmol), ammonium acetate (51.9 mmol) and glacial acetic acid was heated at 100 °C for 20 min under microwave irradiation. Then, 20 ml of water was added and the pH value was adjusted to 7.0 at room temperature.[15–17] The solution was filtered and dried in vacuum to obtain a yellow precipitate. The product was purified in a silicagel column by using ethanol as eluent. (1) Yield, 85.6%; ^{1}H NMR (500 MHz, d_6-DMSO, δ ppm) 9.03 (dd, J = 4.3, 1.7 Hz, 1H), 8.94 (dd, J = 8.1, 1.7 Hz, 1H), 8.32–8.26 (m, 1H), 7.83 (dd, J = 8.1, 4.3 Hz, 1H), 7.64–7.57 (m, 1H), 7.54–7.49 (m, 1H). ^{13}C NMR (d_6-DMSO, δ ppm) 152.65 (s), 149.87 (s), 145.57 (s), 132.06 (s), 131.76 (s), 131.65 (s), 131.05 (s), 128.29 (s), 125.36 (s), 64.81 (s), 58.05 (s). (2) Yield, 87.0%; ^{1}H NMR (500 MHz, d_6-DMSO, δ ppm) 9.06 (dd, J = 4.4, 1.7 Hz, 1H), 8.41 (dd, J = 7.6, 1.2 Hz, 1H), 8.10–8.04 (m, 1H), 7.92 (ddd, J = 8.0, 4.4, 1.7 Hz, 1H), 7.62 (td, J = 7.5, 1.5 Hz, 1H), 7.54 (td, J = 7.6, 1.4 Hz, 1H), 7.22 (s, 1H), 7.12 (s, 1H), 7.02 (s, 1H). ^{13}C NMR (126 MHz, d_6-DMSO, δ ppm) 152.36 (s), 149.40 (s), 146.17 (s), 144.07 (s), 132.90 (s), 131.81 (s), 131.08 (s), 129.87 (s), 128.89 (s), 125.96 (s). 3: Yield, 51.4%; ^{1}H NMR (500 d_6-DMSO, δ ppm) 9.04 (dd, J = 4.3, 1.8 Hz, 1H), 8.92 (d, J = 1.8 Hz, 1H), 8.90 (d, J = 1.8 Hz, 1H), 8.54–8.50 (m, 1H), 8.50–8.48 (m, 1H), 8.17–8.15 (m, 1H), 8.15–8.12 (m, 1H), 7.83 (dd, J = 8.1, 4.3 Hz, 1H). ^{13}C NMR (126 MHz, d_6-DMSO, δ ppm) 150.08 (s), 145.82 (s), 142.88 (s), 136.77 (s), 131.79 (s), 129.84 (s), 128.69 (s), 125.42 (s), 58.04 (s), 45.54 (s). 4: Yield, 81.7%; ^{1}H NMR (500 MHz, d_6-DMSO, δ ppm) 9.04 (dd, J = 4.3, 1.8 Hz, 1H), 8.86 (d, J = 7.3 Hz, 1H), 7.89 (d, J = 1.1 Hz, 1H), 7.87 (d, J = 1.1 Hz, 1H), 7.85 (t, J = 2.6 Hz, 1H), 7.85–7.80 (m, 1H), 7.61 (td, J = 7.5, 1.2 Hz, 1H), 7.56–7.49 (m, 1H). ^{13}C NMR (126 MHz, d_6-DMSO, δ ppm) 151.66 (s), 150.00 (s), 145.64 (s), 135.37 (s), 134.40 (d, J = 8.4 Hz), 133.58 (s), 131.61 (s), 129.93 (s), 125.43 (s), 124.09 (s). 5: Yield, 89.0%; ^{1}H NMR (500 MHz, d_6-DMSO, δ ppm) 9.02 (dd, J = 4.3, 1.8 Hz, 1H), 8.89 (d, J = 1.8 Hz, 1H), 8.88 (d, J = 1.8 Hz, 1H), 8.23–8.21 (m, 1H), 8.21–8.18 (m, 1H), 7.85–7.79 (m, 2H). ^{13}C NMR (126 MHz, d_6-DMSO, δ ppm) 151.50 (s), 149.98 (s), 145.69 (s), 134.08 (s), 131.66 (s), 131.22 (s), 130.12 (s), 125.37 (s), 124.96 (s), 64.81 (s), 58.05 (s).

2.4. Biological activity in vitro

All complexes were dissolved in DMSO with stock solution at 1 mM. Cell viability was determined by measuring the ability of cells to transform MTT to a purple formazan dye.[4] Cells were seeded in 96-well tissue culture plates (3×10^3 cells/well) for 24 h. The cells were then incubated with the tested compounds at different concentrations for 72 h. After incubation, 20 μl/well of MTT solution (5 mg/ml phosphate buffered saline) was added and incubated for 5 h. The medium was aspirated and replaced with DMSO (150 μl/well) to dissolve the formazan salt. The absorbance intensity, which reflects the cell growth condition, was measured at 570 nm using a microplate spectrophotometer (Versamax).

2.5. Drug distribution and location

All complexes were dissolved in DMSO with stock solution at 1 mM. Cells were seeded in 6-well tissue culture plates (5×10^4 cells/well) and were dealted with drugs at 10 μM for 24 h. It's observed that different fluorescence of drugs in cells by using fluorescence microscope (Leica DMI4000B).[18]

2.6. Electronic absorption measurements

UV–vis absorption spectra were recorded on a Shimadzu UV-2550 spectrophotometer by using 1 cm path length quartz cuvettes (3 mL). The absorption titration of the complex **5** in Tris-HCl buffer was performed by using a fixed drug concentration to which increments of the DNA stock solution were added. The concentration of drugs is 20 μM and *c-myc* G4 DNA was added by degrees. Drug-DNA solutions were allowed to incubate for 3 min before the absorption spectra were recorded.

2.7. CD spectra measurements

CD spectra were recorded on a Jasco J810 Circular Dichroism (CD) Spectrophotometer with a thermoelectrically controlled cell

holder. The cell path length was 1 cm.[19] The CD spectra of *c-myc* G4 DNA (2 μM) with the increase of **5** (1 mM) with 2 μL for every 3 min. CD spectra were recorded in the range of 230–600 nm in 0.5 nm increments with an averaging time of 0.5 s.

2.8. FRET melting assays

The fluorescent labeled oligonucleotide, *c-myc* DNA (5′-FAM-TGGGGAGGGTGGGGAGGGTGGGGAAGG-TAMRA-3′, FAM: carboxyfluorescein, TAMRA: 6-carboxytetramethylrhodamine) used as the FRET probes was diluted in Tris-HCl buffer and then annealed by being heated to 92 °C for 5 min, followed by slowly cooling to room temperature. Fluorescence melting curves were determined with a Bio-Radi Q5 realtime PCR detection system, by using a total reaction volume of 25 mL, with labeled oligonucleotide (1 μM) and different concentrations of **5** in Tris-HCl buffer.[9] A constant temperature was maintained for 30 s prior to each reading to ensure a stable value. Final analysis of the data was carried out by using Origin7.5 (Origin Lab Corp.).

2.9. PCR stop assay

The PCR-stop assay was performed by using a modified protocol of the previously reported method. The reactions (40 μL) were performed in 1 × PCR buffer, containing each pair of *c-myc* G4 DNA (10 pM), deoxy nucleotide triphosphate (0.16 mM), Taq polymerase (2.5U), and increasing concentrations of the compound (0–250 μM).[6,9] The reaction mixtures were in cubation in a thermocycler under the following cycling conditions: 94 °C for 3 min followed by 30 cycles at 94 °C for 30 s, 58 °C for 30 s, 72 °C for 30 s. Amplified products were resolved on 15% nondenaturing polyacrylamide gels in 1 × TBE and silver stained.

2.10. Molecular docking study

Automated docking studies were per-formed with three different docking algorithms, AutoDock 3.0 (‘Lamarckian’ genetic algorithm), FlexX 1.10 (incremental construction algorithm, as implemented in Sybyl 6.8), and GOLD 1.2 (‘Darwinian’ genetic algorithm). As scoring is a very important second aspect of automated docking method-ologies, it was decided to investigate the effect of rescoring: the process of reprioritization of docking solutions (primarily ranked by the ‘native’ scoring function implemented in the docking program) with an additional stand-alone scoring function.

3. Results and discussion

3.1. Biological activity

The antitumor activity of synthetic phenanthroimidazole derivatives against MDA-MB-231 highly metastatic human breast adenocarcinoma cells and MCF-7 lowly metastatic human breast cancer cells, and cervical cancer Hela cells was evaluated by MTT assay, as shown in Table 1. It’s found that all of these compounds, exhibit certain inhibition to various tumor cells after 72 h treatment, especially **4** and **5** displayed great antitumor activity. The inhibitory activity (IC_{50}) of **5** against MDA-MB-231 cells is about 3.6 μM, which is far more less to that of *cis*-platin (36.1 μM). These results shown that phenanthroimidazole derivatives can effectively inhibit the growth of tumor cells, and the para-orienting complex exhibits better antitumor activity than ortho-orienting.

Table 1
The inhibitory activity (IC_{50}/μM) of the target compounds and *cis*-platin against human breast cancer cells.

Compd	Inhibitory activity/IC_{50} (μM)		
	MDA-MB-231	MCF-7	Hela
1	74.2	72.6	5.1
2	152.3	161.9	240.3
3	60.0	184.3	62.4
4	36.0	27.3	7.9
5	3.6	22.9	8.5
cis-platin	36.1	3.0	9.4

3.2. Drug distribution and location

As shown in Figure 2B, a number of MCF-7 cells were shrinking to globe after dealt with **5** at 10 μM for 24 h. It’s observed that there are less than 20% cell membrane surface become rough and uneven with large and more particles, the cell membrane structure is incomplete. Especially, the cell surface obviously appeared numerous holes and displayed the obvious characteristics of apoptosis of MCF-7 cells. Besides, **5** entered into MCF-7 cells and exhibited green and blue flurensence, which was located and distributed in cell cytoplasm and nucleus. As shown in Figure 2A, the flurensence observation for **4** was also found that **4** also exhibited green and blue flurensence, which displayed similar activity with **5**. Compounds **1**–**3** with little fluorescence was observed, complex **4** and **5** can be uptook by MCF-7 cells and glowing strong green and blue fluorescence, a possible reason is mainly due to the absence of hyperchrome Br atom.

3.3. Electronic titration

Considering *c-myc* oncogene plays a key role in the proliferation, apoptosis, invasion and metastasis of tumor cells, the interaction of complex **5** with *c-myc* G-quadruplex DNA has been investigated as a promising target for anti-tumor agent.

Electronic spectra titration are one of the most common methods to evaluate the interaction of small molecules with biology macromolecules, which are conducted to confirm whether **5** can bind to *c-myc* G4 DNA. In general, small molecules exhibit characteristic absorption in electronic spectra which will undergo hypochromism and red shift in the presence of biology molecules and the degree of change depend on the binding affinity.[20]

As shown in Figure 3A, the electronic spectra of **5** in Tris-HCl buffer(pH = 7.2) solution exhibit the characteristic IL (intraligand charge transfer) absorption in the range of 250–300 nm with the maximum at 274 nm. When *c-myc* G4 DNA was added into the solutions, obvious hypochromism and red shift was observed. The hypochromism at IL absorption is about 9.4% ($\Delta\lambda$ = 2.5 nm), indicating that **5** can bind to *c-myc* G4 DNA.

3.4. Circular dichroism spectra

Circular dichroism (CD) spectra, which is a powerful stool to investigate the conformation change of biology molecules, was been further carried out to confirmed the binding of **5** with *c-myc* G4 DNA, as shown in Figure 3B. In general, G-quadruplex DNA will exhibit a positive CD signal in the range of 250–300 nm, with the maximum at 264 nm.[21] Upon the addition of **5**, the decreased signals of *c-myc* G4 DNA in the CD spectra were observed. The CD signal for *c-myc* G4 DNA at 264 nm gradually receded with the addition of **5** and the CD signal strengths decreased 23.0%. The change is in consistent with the induction of the guanine-rich DNA to form the G-quadruplex DNA structure by compound, and the results has been treated as evident of

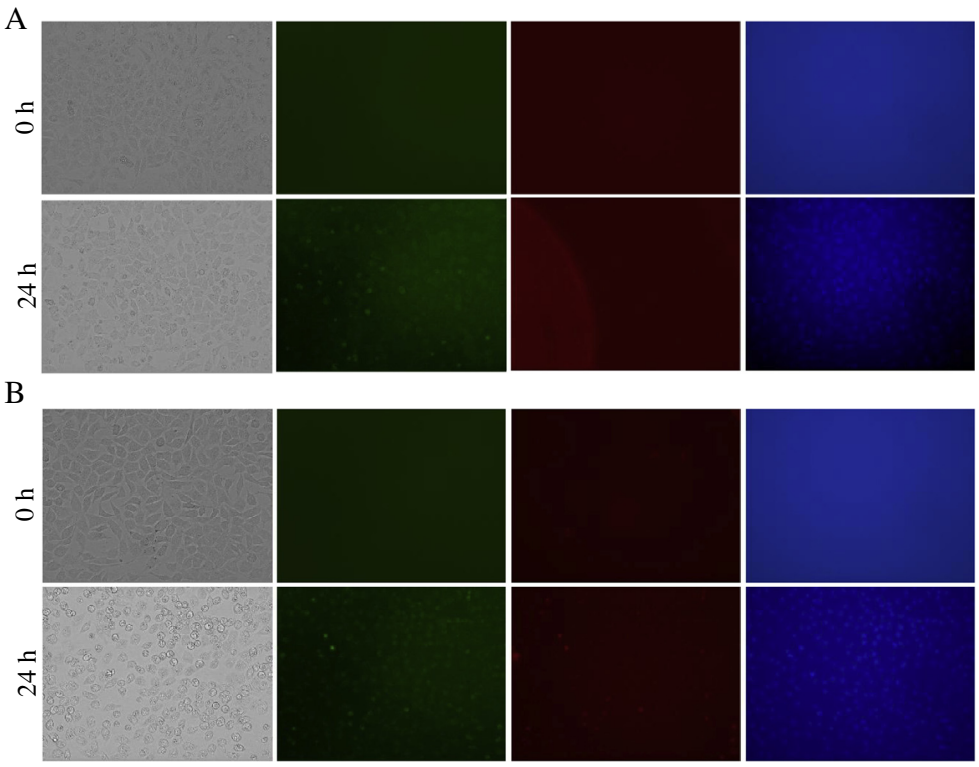

Figure 2. The distribution and location of complex **4** (A) and **5** (B) in MDA-MB-231 cells by using fluorescence microscope.

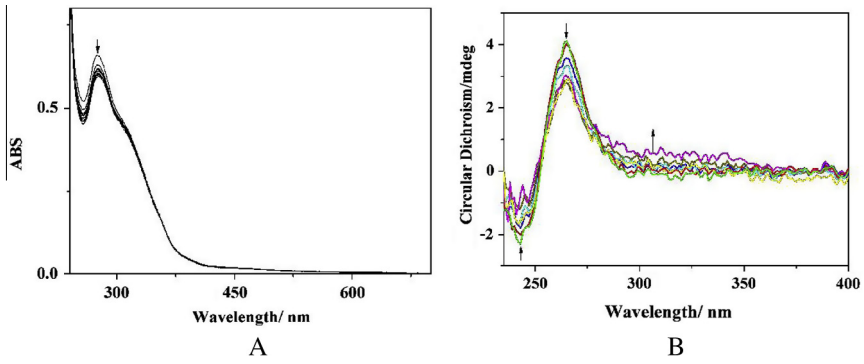

Figure 3. (A) The electronic spectra of **5** in absence and in presence of *c-myc* G-quadruplex DNA. [**5**] = 5×10^{-5} M, [*c-myc* G-quadruplex DNA] = (0–40) $\times 10^{-4}$ M. Arrow shows the absorbance changing upon increasing *c-myc* G-quadruplex DNA concentrations. (B) The CD spectra of *c-myc* G-quadruplex DNA in the absence and presence of increasing amounts of **5**. [*c-myc* G-quadruplex DNA] = 2×10^{-6} M, [**5**] = (0–118) $\times 10^{-6}$ M. Arrow shows the absorbance changing upon increasing **5**.

binding behavior for the ligand and indicated that the G-quadruplex DNA structure was stabilized by ligand **5**.

3.5. FRET melting point curves

To investigate the thermodynamic stability of the *c myc* G4 DNA with **5**, a FRET melting point assay was carried out to detect the melting temperature.

As shown in Figure 4A, the melting point[8] of *c-myc* G4 DNA is about 43.8 °C, upon the addition of 1.0 and 3.0 μM of **5**, the T_m increased to 47.2 (ΔT_m = 3.4) and 50.2 (ΔT_m = 6.4) °C, respectively. Moreover, the melting point of the concentration -dependent melting curves of **5** are showed in Figure 4B. It is found that all of the ΔT_m values of the samples incubated with **5** increased compared with the control value, indicating that **5** could enhance the thermodynamic stability of *c-myc* oligomer.[22]

3.6. Molecular docking

Molecular docking study was performed to investigate the possible binding interaction between **5** and *c-myc* G-quadruplex DNA. The conformation with the lowest binding energy (−8.04 kcal/mol) was selected as the best binding conformation from the first cluster including 64 docking conformations.[7] The binding energy is made up of two components, intermolecular energy (−8.34 kcal/mol) and torsional energy (0.30 kcal/mol), and intermolecular energy is contributed by two parts as follows: the sum (−8.38 kcal/mol) of van der Waals energy, hydrogen bond energy and desolvation energy, and the electrostatic energy (0.04 kcal/mol). In addition, **5** is hydrophobic with *C*Log*P* = 4.66 calculated by ChemBioDraw software. This property just suits to the corresponding hydrophobic environment inside the G-quadruplex DNA. Therefore, the van der Waals interactions between

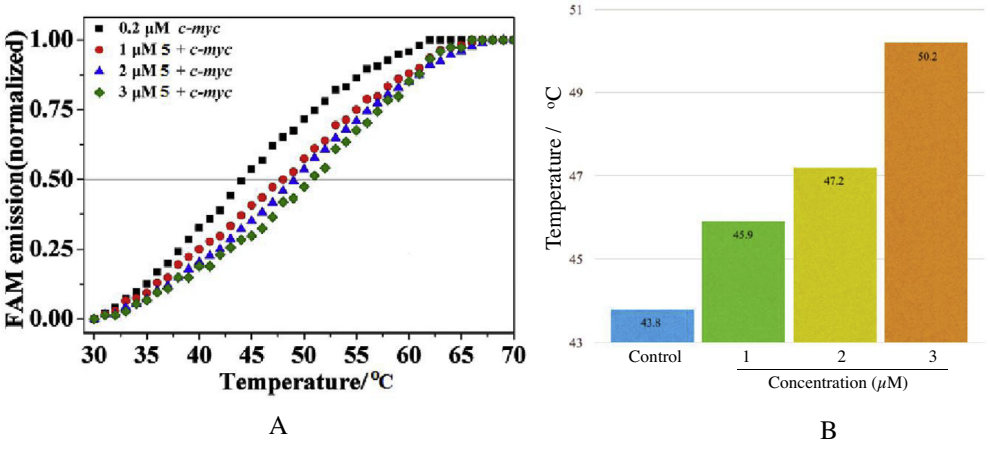

Figure 4. (A) FRET melting profiles of 0.2 μM *c-myc* G-quadruplex DNA with **5**; (B) The melting rising trend with the increasing of **5**.

5 and *c-myc* G4 DNA may play a dominating role in binding affinity.

Herein, a complete overview of docking binding mode of **5** to *c-myc* G4 DNA is presented in Figure 5. It can be clearly seen that the planarity **5** is suitably stacking onto the 5′G-quartet surface. Compound **5** is largely in the same plane with A6, and it respectively parallels to the surfaces of the G5 and G-quartet consisting of G7, G11, G16, and G20. Thus, π–π stacking interactions exist presumably between **5** and the two surfaces to enhance the binding affinity. These docking results reasonably explain our

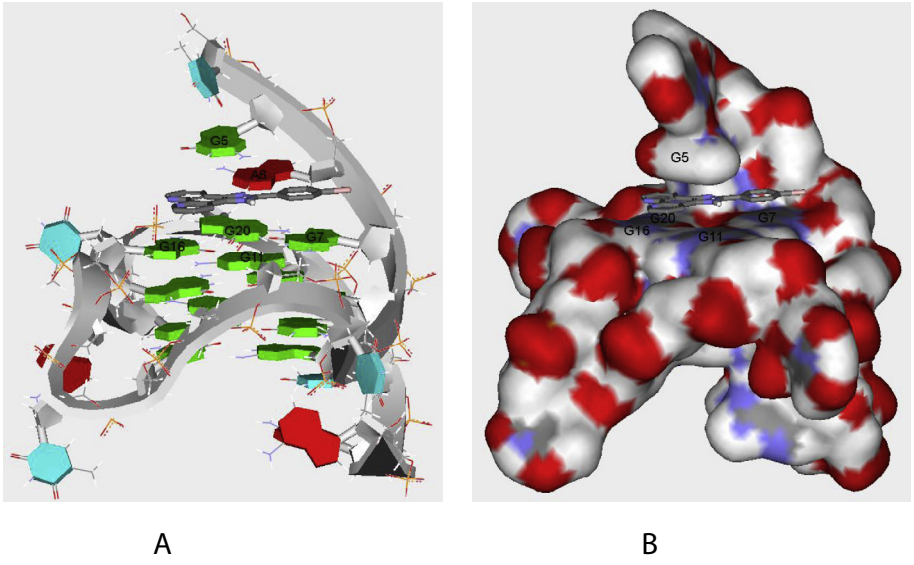

Figure 5. (A) The binding mode between **5** and *c-myc* G-quadruplex DNA predicted by docking. (B) Docking conformation of **5** and corresponding surface of *c-myc* G-quadruplex DNA, in which the red and blue regions represent oxygen and nitrogen atoms respectively, whereas grey and white regions represent carbon and hydrogen atoms.

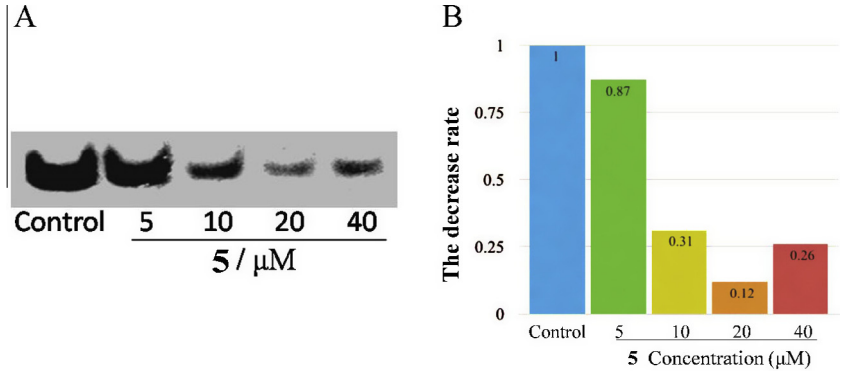

Figure 6. Effect of **5** on the hybridization of *c-myc* G-quadruplex DNA in the PCR-stop assay, [**5**] = 0.0–40 × 10^{-6} M.

experimental fact that **5** could bind to *c-myc* G4 DNA in intercalating mode.

3.7. PCR-stop

PCR-stop assay have also been conduct to determine whether these complexes were inhibit the activity of Taq polymerase by stabilizing the G-quadruplex DNA structure of tested oligomer. In the presence of some G-quadruplex DNA stabilizers, the template sequence was induced into a G-quadruplex DNA structure that blocked the hybridization and the detection of the final PCR product. And the result was illustrated in Figure 6.

As shown in Figure 6, the single strand *c-myc* G-quadruplex DNA will hybrid with a complementary strand in the presence of Taq polymerase (Control). When **5** was added into the solution, a G-quadruplex DNA structure was induced to block the hybridization with a complementary strand. What's more, the inhibitory effect increased with increasing concentration.[4,5] As a result, the 5′–3′ extension with Taq polymerase was inhibited and double-stranded DNA PCR product was decreased.

4. Conclusions

In conclusion, a series of phenanthroimidazole derivatives have been prepared in average yield range of 50–80% under microwave irradiation. It's found that these compounds can effectively inhibit the growth of tumor cells, especially **5** exhibit the best antitumor activity against MDA-MB-231 cells. Further studies indicated that **5** can interact and stabilize the G-quadruplex structure of *c-myc*. In addition, the molecular docking calculation suggested that **5** may bind to the base pair through π–π stacking, as a result to block the replication of *c-myc* oligomer. In a word, these studies not only offer the reliable binding behavior of **5** with *c-myc* G4 DNA but also provide insights into the possible anticancer mechanism at molecular level, and thus they will lay the foundation for the rational design of new compounds with higher affinity to *c-myc* G-quadruplex DNA.

Acknowledgments

We are pleased to thank the financial support of the Natural Science Foundation of Guangdong Province (S2011040000131), Name of the Science and Technology Foundation of Guangdong Province (20070327029), Guangdong Province Science and Technology Plan (20771044), Guangzhou City Science and Technology Plan (2011J5200017), Medical Science and Technology Research Foundation of Guangdong Province (WSTJJ20101231), Science and Technology Project of Guangzhou (2012J2200034, 2013J4100072), Science Research Program of Guangzhou Municipal Colleges (2012C219) and Foundation of Guangzhou Medical University (2010C15). Project supported by The Joint Natural Sciences Fund of The Department of Science and Technology and The First Affiliated Hospital of Guangdong Pharmaceutical University (GYFYLH201309).

Supplementary data

Supplementary data associated with this article can be found, in the online version, at http://dx.doi.org/10.1016/j.bmc.2014.09.003.

References and notes

1. Dang, C. V. *Cell* **2012**, *149*, 22.
2. Dang, C. V.; Le, A.; Gao, P. *Clin. Cancer Res.: Official J. Am. Assoc. Cancer Res.* **2009**, *15*, 6479.
3. Dominguez-Sola, D.; Ying, C. Y.; Grandori, C.; Ruggiero, L.; Chen, B.; Li, M.; Galloway, D. A.; Gu, W.; Gautier, J.; Dalla-Favera, R. *Nature* **2007**, *448*, 445.
4. Wu, P.; Ma, D. L.; Leung, C. H.; Yan, S. C.; Zhu, N.; Abagyan, R.; Che, C. M. *Chemistry* **2009**, *15*, 13008.
5. Wang, P.; Leung, C. H.; Ma, D. L.; Yan, S. C.; Che, C. M. *Chemistry* **2010**, *16*, 6900.
6. Ou, T.-M.; Lu, Y.-J.; Zhang, C.; Huang, Z.-S.; Wang, X.-D.; Tan, J.-H.; Chen, Y.; Ma, D.-L.; Wong, K.-Y.; Tang, J. C.-O. *J. Med. Chem.* **2007**, *50*, 1465.
7. Ma, D.-L.; Chan, D. S.-H.; Fu, W.-C.; He, H.-Z.; Yang, H.; Yan, S.-C.; Leung, C.-H. *PLoS One* **2012**, *7*, e43278.
8. Grand, C. L.; Han, H.; Muñoz, R. M.; Weitman, S.; Von Hoff, D. D.; Hurley, L. H.; Bearss, D. J. *Mol. Cancer Ther.* **2002**, *1*, 565.
9. Ma, Y.; Ou, T. M.; Hou, J. Q.; Lu, Y. J.; Tan, J. H.; Gu, L. Q.; Huang, Z. S. *Bioorg. Med. Chem.* **2008**, *16*, 7582.
10. Hoffman, B.; Liebermann, D. A. *Oncogene* **2008**, *27*, 6462.
11. Sun, D.-D.; Wang, W.-Z.; Mao, J.-W.; Mei, W.-J.; Liu, J. *Bioorg. Med. Chem. Let.* **2012**, *22*, 102.
12. Preti, L.; Attanasi, O. A.; Caselli, E.; Favi, G.; Ori, C.; Davoli, P.; Felluga, F.; Prati, F. *Eur. J. Org. Chem.* **2010**, *2010*.
13. Kumari, S.; Bugaut, A.; Huppert, J. L.; Balasubramanian, S. *Nature Chem. Biol.* **2007**, *3*, 218.
14. Freyer, M. W.; Buscaglia, R.; Kaplan, K.; Cashman, D.; Hurley, L. H.; Lewis, E. A. *Biophys. J.* **2007**, *92*.
15. Steenackers, H.; Ermolat'ev, D.; Trang, T. T.; Savalia, B.; Sharma, U. K.; De Weerdt, A.; Shah, A.; Vanderleyden, J.; Van der Eycken, E. V. *Org. Biomol. Chem.* **2014**, *12*, 3671.
16. Zhang, Z.; Wang, Q.; Wu, Q.; Hu, X. Y.; Wang, C. X.; Mei, W. J.; Tao, Y. Y.; Wu, W. L.; Zheng, W. J. *Chem. J. Chin. Univ.* **2012**, *33*, 2441.
17. Fantini, M.; Zuliani, V.; Spotti, M. A.; Rivara, M. *J. Comb. Chem.* **2010**, *12*, 181.
18. Bae, Y.; Nishiyama, N.; Fukushima, S.; Koyama, H.; Yasuhiro, M.; Kataoka, K. *Bioconjugate Chem.* **2005**, *16*, 122.
19. Gray, D. M.; Wen, J. D.; Gray, C. W.; Repges, R.; Repges, C.; Raabe, G.; Fleischhauer, J. *Chirality* **2008**, *20*, 431.
20. Bhattacharjee, A. J.; Ahluwalia, K.; Taylor, S.; Jin, O.; Nicoludis, J. M.; Buscaglia, R.; Brad Chaires, J.; Kornfilt, D. J.; Marquardt, D. G.; Yatsunyk, L. A. *Biochimie* **2011**, *93*, 1297.
21. Fan, C.; Wu, Q.; Chen, T.; Zhang, Y.; Zheng, W.; Wang, Q.; Mei, W. *Med. Chem. Commun.* **2014**, *5*, 597.
22. Wu, Q.; Chen, T.; Zhang, Z.; Liao, S.; Wu, X.; Wu, J.; Mei, W.; Chen, Y.; Wu, W.; Zeng, L.; Zheng, W. *Dalton Trans.* **2014**, *43*, 9216.